

## Satellite remote sensing of changes in NO<sub>x</sub> emissions over China during 1996–2010

ZHANG Qiang<sup>1\*</sup>, GENG GuanNan<sup>1,2</sup>, WANG SiWen<sup>2</sup>, RICHTER Andreas<sup>3</sup> & HE KeBin<sup>2</sup>

<sup>1</sup> Ministry of Education Key Laboratory for Earth System Modeling, and Center for Earth System Science, Tsinghua University, Beijing 100084, China;

<sup>2</sup> State Key Joint Laboratory of Environment Simulation and Pollution Control, School of Environment, Tsinghua University, Beijing 100084, China;

<sup>3</sup> Institute of Environmental Physics, University of Bremen, Bremen 28359, Germany

Received October 31, 2011; accepted December 27, 2011; published online March 8, 2012

Satellite derived NO<sub>2</sub> column data have been used to study Chinese national fossil fuel consumption and pollutant emissions. Based on NO<sub>2</sub> retrievals from two satellites (GOME and SCIAMACHY) for 1996–2010, we analyzed the characteristics and evolution of regional pollution related to NO<sub>x</sub> emissions in China. Satellite observations indicated that the highly polluted regions were expanding. Anthropogenic emission dominated areas have expanded from the east to central and western China, and new highly polluted regions have formed throughout the nation. Bottom-up emission estimates suggested a 133% increase in anthropogenic NO<sub>x</sub> emissions in East Central China during 1996 to 2010, which was lower than the 184% increase of the NO<sub>2</sub> columns measured by the satellites. We found that growth rates of NO<sub>x</sub> emissions have slowed in Chinese megacities over recent years, in contrast to which, the NO<sub>x</sub> emissions were soaring in medium-sized cities, indicating that strict controls of NO<sub>x</sub> emissions from coal-fired facilities are required in China.

**NO<sub>x</sub>, satellite remote sensing, SCIAMACHY, regional pollution, urban expansion**

**Citation:** Zhang Q, Geng G N, Wang S W, et al. Satellite remote sensing of changes in NO<sub>x</sub> emissions over China during 1996–2010. *Chin Sci Bull*, 2012, 57: 2857–2864, doi: 10.1007/s11434-012-5015-4

Nitrogen oxides (NO<sub>x</sub> = NO + NO<sub>2</sub>) are major contributors to regional air pollution. NO<sub>x</sub> is released into the atmosphere as a result of anthropogenic (e.g. fossil fuel combustion) and natural (e.g. soil emissions, lightning, biomass burning) processes. They are important precursors of tropospheric ozone and aerosols, and also participate in the formation of acidic precipitation; hence, they are detrimental to human health and the ecosystem. During the past two decades, China has experienced rapid economic growth, converting the world's largest agrarian nation into an industrial society. This process is driven by fossil fuel consumption, and large volumes of air pollutants are released into the atmosphere, leading to a series of complex air pollution problems such as acid rain, haze, and photochemical smog [1,2]. NO<sub>x</sub> emission has a close relationship with fossil fuel consump-

tion, and subsequently in China over the last 20 years, NO<sub>x</sub> has increased the most rapidly of any air pollutant [3–5].

An accurate understanding of the complex regional air pollution largely depends on the quantification of a priori emissions. Previous studies focused on emission budgets and spatial-temporal distributions of air pollutants, are mainly based on bottom-up emission inventory data [3,5,6]. However, this method is only as accurate as the statistical data and local emission factors [5] used in the calculation. Recently developed space-borne remote sensing technology provides an alternative and effective approach to the quantification of air pollutants [7,8]. Among the various species amenable to satellite observation, NO<sub>2</sub> has been studied the most broadly [9–13]. This is because: (1) retrieval of NO<sub>2</sub> is less affected by the other strongly absorbing atmospheric species; and (2) NO<sub>2</sub> has a short atmospheric lifetime, which allows closer linking of the measured NO<sub>2</sub> columns to the

\*Corresponding author (email: qiangzhang@tsinghua.edu.cn)

surface emissions of  $\text{NO}_x$  [10,14,15]. The anthropogenic  $\text{NO}_x$  emissions are mainly produced alongside energy use, so that  $\text{NO}_2$  in polluted regions is a good indicator of fossil fuel consumption [16].

In this study, we used satellite derived tropospheric  $\text{NO}_2$  columns to study the spatial-temporal variations of  $\text{NO}_x$  emissions between 1996 and 2010 in China, and investigated the forcing factors of these changes.

## 1 Data and methods

### 1.1 Instruments and data

Since 1996, several space-borne instruments have been launched to observe tropospheric  $\text{NO}_2$  columns, including the Global Ozone Monitoring Experiment (GOME, 1996–2002), the Scanning Imaging Absorption Spectrometer for Atmospheric Cartography (SCIAMACHY, 2003 to present), the Ozone Monitoring Instrument (OMI, 2005 to present), and the Global Ozone Monitoring Experiment-2 (GOME-2, 2007 to present). GOME, SCIAMACHY, and GOME-2 have local passing times over China between 9:30 and 10:30 am, and, partly because of the similar algorithms used to retrieve the data, these measurements have been shown to have high consistency [10]. However, serious instrument degradation in GOME-2 since 2009 means it cannot now be used for trend analysis [17]. Although OMI has the higher spatial resolution of the four instruments, it has an early afternoon local passing time, which makes it difficult to directly compare to the others. In this work GOME measurements from April 1996 to the end of 2002 were used, and SCIAMACHY measurements from 2003 to 2010.

GOME and SCIAMACHY are both sponsored by the European Space Agency. GOME was launched in April 1995 on board the ERS-2 satellite and was the first space-borne instrument designed to measure the precursors of lower tropospheric ozone and other trace gases. SCIAMACHY was launched in March 2002 on board the ENVISAT-1 platform. Both of these instruments are passive remote sensing spectrometers. GOME measures the earthshine radiance and the solar irradiance in the UV/VIS spectral range (240–790 nm) at a spectral resolution of 0.2–0.4 nm and a nadir pixel size of 320 km  $\times$  40 km. With a 960 km across-track swath width, the global coverage by GOME can be achieved per three days (daily coverage achieved above 65° latitudes) [18]. SCIAMACHY measures the spectral ranged from 240 to 2380 nm, covering the near-infrared wavelength. The nadir pixel size for SCIAMACHY is about 60 km  $\times$  30 km, and the spectral resolution is 0.22–1.48 nm. Global coverage is achieved every 6 days by SCIAMACHY [19].

### 1.2 Methodology

In this study, we use the GOME and SCIAMACHY tropospheric  $\text{NO}_2$  column products retrieved by the Institute of

Environmental Physics, Bremen University. The retrieval process consists of three steps [10]: First, a slant  $\text{NO}_2$  column density is determined from a spectral fit using a Differential Optical Absorption Spectroscopic (DOAS) approach at 425–450 nm. Then the stratospheric contribution to the slant columns is estimated by assimilating slant columns provided by the SLIMCAT model and then removed from the total slant column. Finally, the residential tropospheric slant column is converted into vertical column by application of the tropospheric air mass factor (AMF) calculated by SCIATRAN. For individual retrievals, the absolute error attributed to the random spectral fit and subtraction of the stratospheric contribution is estimated to be  $(0.5\text{--}1.0) \times 10^{15}$  molecules  $\text{cm}^{-2}$ . The relative error in the month-average column is 40%–60% in polluted regions, largely because of the AMF uncertainty (not important for trend analyses). The overall error of the annual change in the  $\text{NO}_2$  column over China is estimated to be 15% [10].

The accuracy of the satellite measurements is reduced by clouds, which block the observation of  $\text{NO}_2$  beneath them. The satellite pixels showing cloud fraction  $>0.2$  were filtered out in our analysis. Cloud information is synchronously derived from the observations of GOME and SCIAMACHY, which is available from the website of the Royal Netherlands Meteorological Institute (<http://www.temis.nl/fresco/>). We then allocated the swath data into  $0.125^\circ \times 0.125^\circ$  horizontal grids and calculated the month-average  $\text{NO}_2$  columns for each grid.  $\text{NO}_x$  has a shorter lifetime in summer so that will be transported less far from sources than in winter. Therefore, the observed  $\text{NO}_2$  columns have the closest relationship to surface  $\text{NO}_x$  emissions in summer [4]. For this reason we used the summer average  $\text{NO}_2$  columns to demonstrate the spatial characteristics of the emissions, and to analyze the temporal trend based on the annual average  $\text{NO}_2$  columns.

## 2 Results

### 2.1 Spatial-temporal variations of $\text{NO}_2$ columns during 1996–2010

Figure 1 shows the spatial-temporal variations of  $\text{NO}_2$  columns observed by the satellites during 1996–2010 in East Central China. Using only summer satellite measurements, these observations show significant characteristics of regional pollution, with greater spatial coverage of highly polluted areas. During 1996–1998, these regions of high  $\text{NO}_x$  emissions were mainly concentrated in the North China Plain, Yangtze River Delta, and Pearl River Delta. However, by 2008–2010, the  $\text{NO}_x$  emission strengths in these areas had increased, resulting in super-regions of pollution including Beijing-Tianjin-Tangshan, Central of Hebei, West of Shandong, and North Central of Henan. The extension of high polluted regions in Yangtze River Delta also enlarged. In addition, new hotspots appeared in Jilin, Central Liaoning,

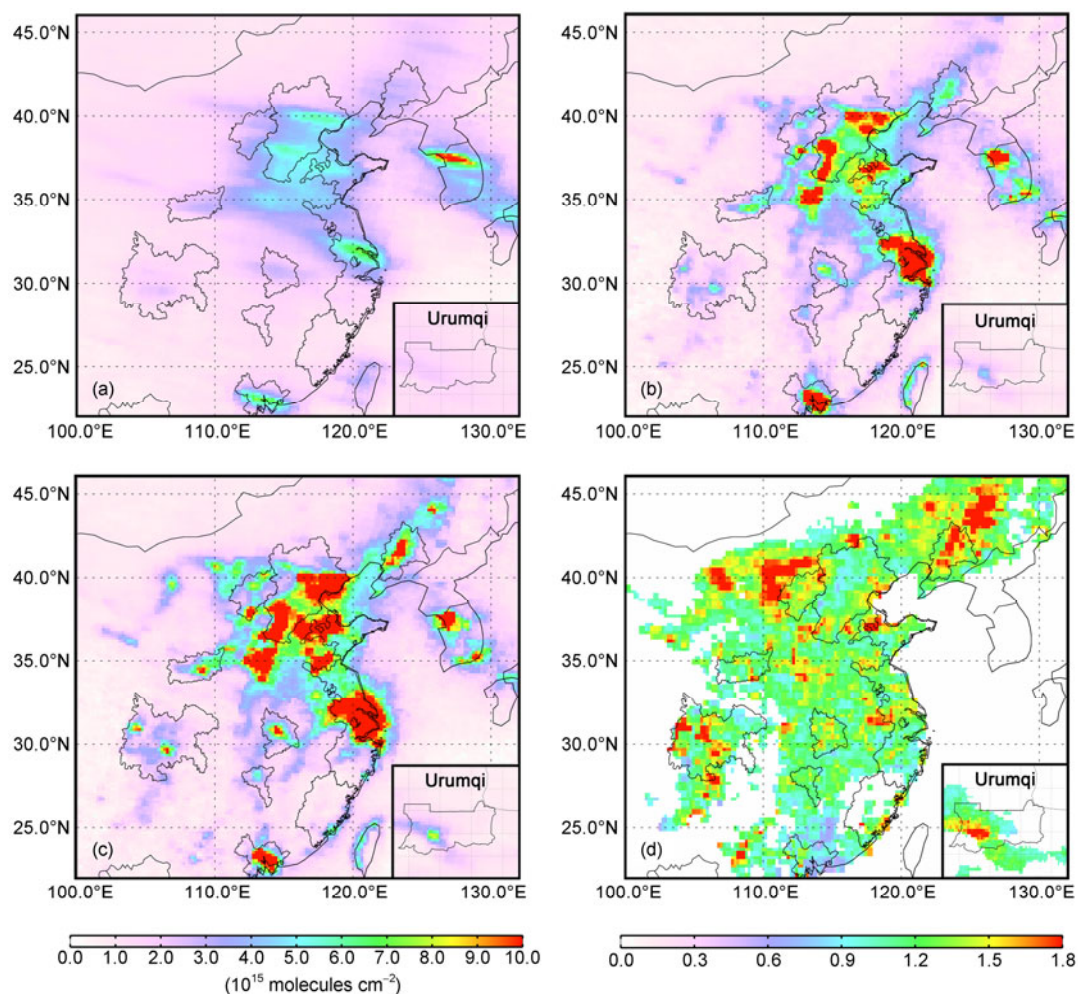


**Figure 1** Satellite observed spatial-temporal variations of  $\text{NO}_2$  columns during 1996 to 2010. Solid lines within the Chinese national boundaries denote the twelve key regions defined in the “Joint Prevention and Control Strategy” by Ministry of Environmental Protection (MEP). (a) Summer average tropospheric  $\text{NO}_2$  columns retrieved from GOME for the period 1996 to 1998. (b) Summer average tropospheric  $\text{NO}_2$  columns retrieved from SCIAMACHY for the period 2003 to 2005. (c) Summer average tropospheric  $\text{NO}_2$  columns retrieved from SCIAMACHY for the period 2008–2010. (d) Ratios of (c) and (b). Grids with tropospheric  $\text{NO}_2$  columns less than  $10^{15}$  molecules  $\text{cm}^{-2}$  are not colored in (d).

Inner Mongolia, North Central Shanxi, Guanzhong Zone in Shaanxi, the Wuhan City cluster, Chengdu-Chongqing, and the Urumqi City cluster.

Figure 2 shows the changes in tropospheric  $\text{NO}_2$  columns between 2000 and 2010 in three differently sized city-clusters: Beijing-Tianjin-Tangshan, Wuhan and surroundings, and the city-cluster in South Shandong. By 2010, the high  $\text{NO}_2$  columns covered the entire urban areas in these three regions. We also found that the growth rates of  $\text{NO}_x$  emissions and pollution levels in medium-sized cities such as Zaozhuang, Linyi, and Jining were comparable to those in the megacities, indicating the urgency of implementing controls on  $\text{NO}_x$  emissions in medium-sized Chinese cities.

With the increase of serious regional pollution in China, the General Office of State Council published the “Guiding Opinions on Facilitating the Joint Prevention and Control of Air Pollution and Improving the Regional Air Quality”. This was issued by nine ministries including MEP, and aims

to facilitate the joint control of regional pollution in nine (later 12) key regions [20]. Figure 1 shows the three economic circles (Beijing-Tianjin-Hebei, Yangtze River Delta, and Pearl River Delta), and the nine city-clusters (Central of Liaoning Province, Shandong Peninsula, the Wuhan City cluster, Changsha-Zhuzhou-Xiangtan, Chengdu-Chongqing, West Coast of Taiwan Strait, West and Central Shanxi Province, Guanzhong zone in Shaanxi Province, and the Urumqi City cluster). Satellite observations between 2008 and 2010 suggested that these key regions marked by MEP in the “Joint Control and Prevention Strategy” cover the main high  $\text{NO}_x$  emission areas. Therefore, these key regions are representative; however, the highly polluted city-clusters in Central of Henan and West of Shandong are not included in the Strategy, and the rapid growth in  $\text{NO}_x$  emissions from industrial regions in Jilin and Inner Mongolia risks turning these two provinces into new highly polluted areas. We suggest considering these regions as top priorities in the

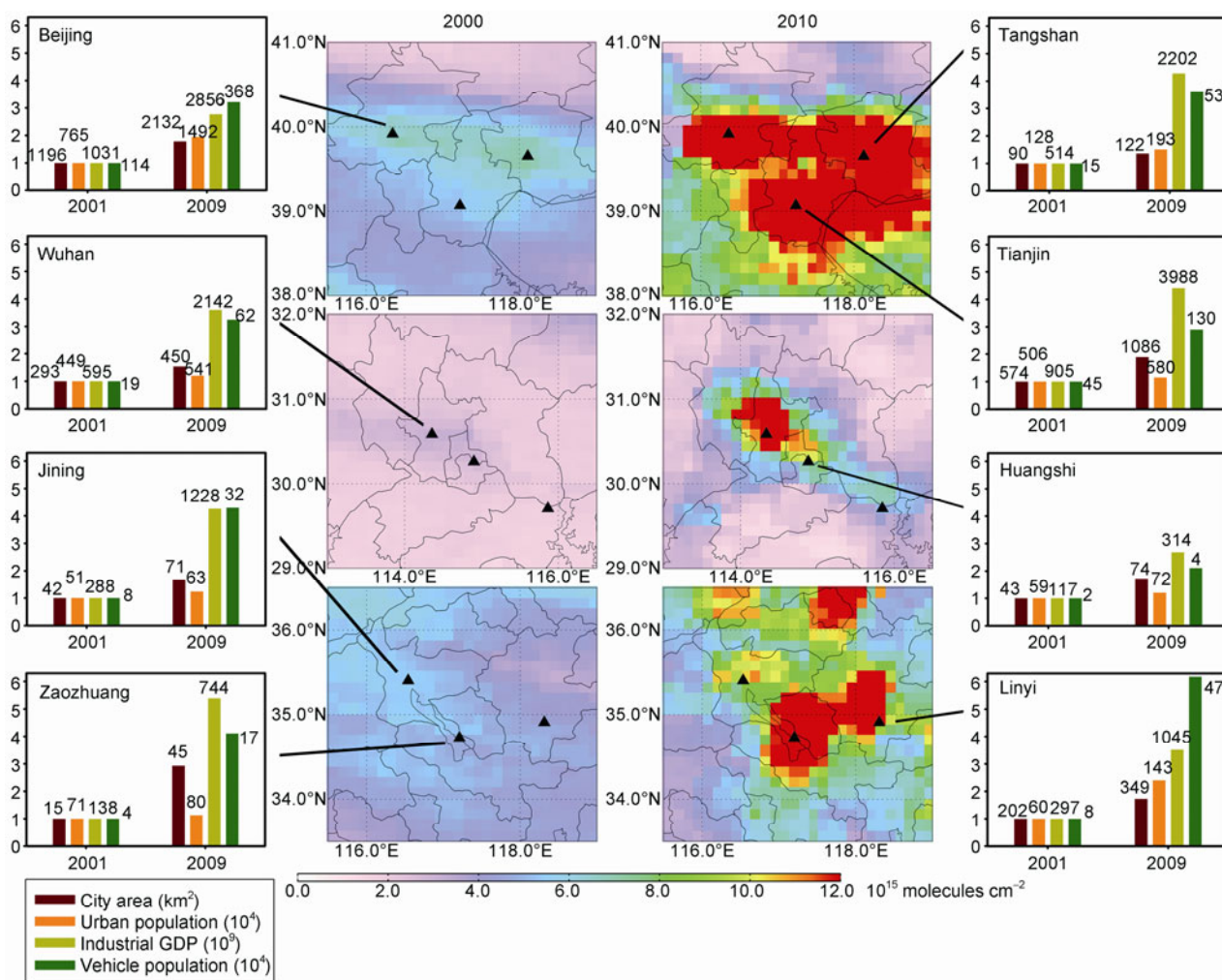


**Figure 2** Changes in tropospheric NO<sub>2</sub> columns and the major socio-economic indexes of three city clusters between 2000 and 2010. From top to bottom: Beijing-Tianjin-Tangshan, Wuhan and surroundings, and the city-cluster in South Shandong.

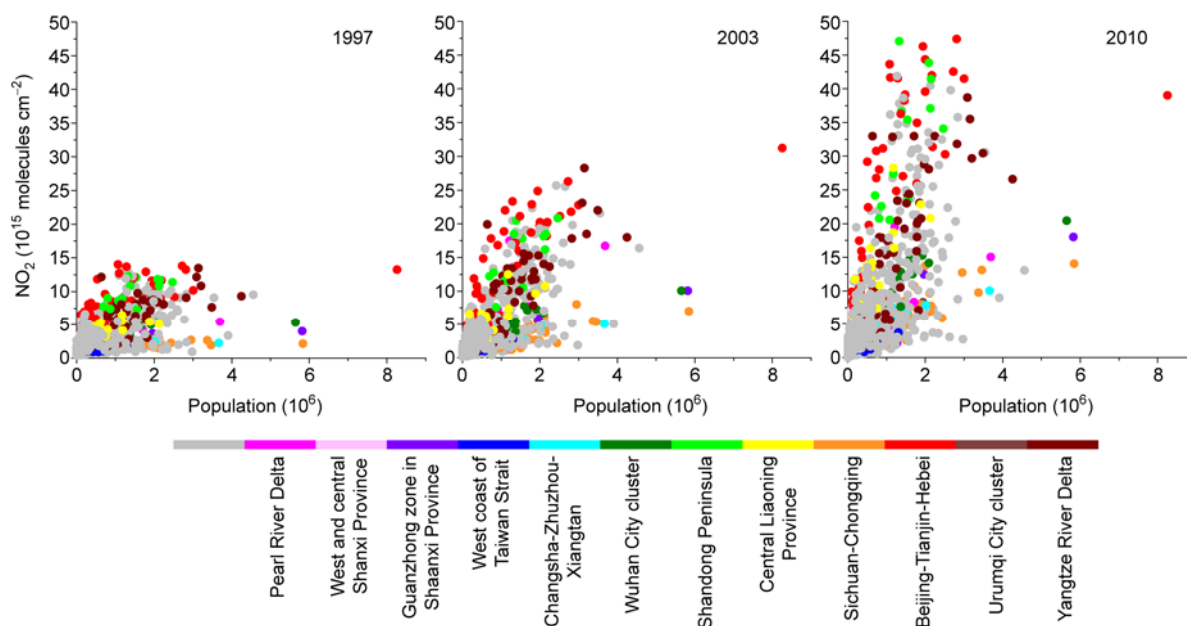
next stage of the strategy.

In the past decade, the growth rates of NO<sub>2</sub> columns in Beijing-Tianjin-Hebei, Shandong Peninsula and Yangtze River Delta stand out among these key regions (Figure 3). Correlation analysis between the NO<sub>2</sub> columns and the population density indicates a slowing down of the growth rates of the NO<sub>2</sub> columns in the megacities during 2008–2010. This contrasts with the rapid growth of the same in medium sized cities. Figure 4 shows the profiles and evolution of the summer average tropospheric NO<sub>2</sub> columns over three typical latitude bands. The growth rate of NO<sub>2</sub> columns between 2003 and 2010 is smaller than that between 1997 and 2003 over Shanghai, but the high polluted areas have extended. In contrast, the growth rates of NO<sub>2</sub> columns in medium sized cities such as Wuhan, Handan, Zibo, and Zunyi between 2003 and 2010 are larger than those between 1997 and 2003. Similar results are also found over other latitude bands, which can be characterized as the growth of NO<sub>2</sub> columns in megacities mainly occurred in the first half of the period during 1996–2010, while the NO<sub>2</sub> columns in

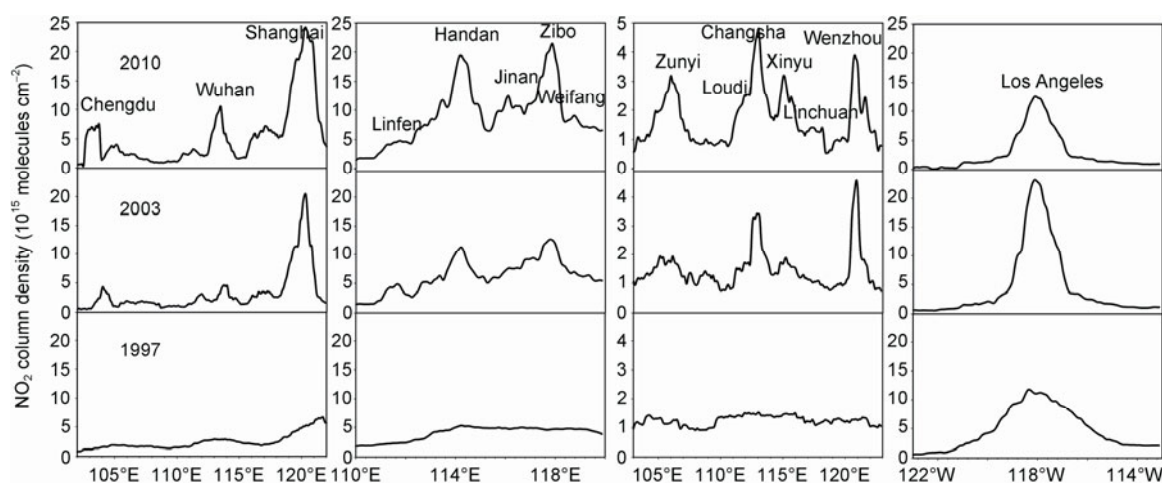
medium sized cities have increased more significantly in recent years. It is worth noting that direct comparison of GOME and SCIAMACHY at high-resolution grid level are qualitative because of the differences in spatial resolution between two instruments.

Figure 1(d) shows the growth rates of NO<sub>x</sub> emissions in different regions over the past five years. To minimize uncertainties, the grids with summer average NO<sub>2</sub> columns lower than 10<sup>15</sup> molecules cm<sup>-2</sup> have been removed. We found the most rapid growth of NO<sub>x</sub> emissions occurred in the old industrial regions in Jilin and Liaoning, and newly developing industrial regions in Inner Mongolia, Shanxi, and Ningxia. The growth of NO<sub>x</sub> emissions has slowed down in megacities such as Beijing, Shanghai, and Guangzhou.

In regions dominated by anthropogenic emissions, tropospheric NO<sub>2</sub> columns show winter maxima, because of the longer lifetime of NO<sub>x</sub> and the less turbulent conditions in winter. In regions dominated by emissions from natural sources such as soils and lightning, the emission strength is



**Figure 3** Correlations between the  $\text{NO}_2$  columns and the population density in twelve key regions during 1997–2010. Data are at  $0.5^\circ \times 0.5^\circ$  grids. Colors denote different regions. Grey data are for grids outside the twelve key regions.



**Figure 4** Profiles and evolution of summer average tropospheric  $\text{NO}_2$  columns in three typical latitude bands during 1997–2010.

far higher in summer so that the tropospheric  $\text{NO}_2$  columns show summer maxima. These seasonal characteristics can be used to identify the dominant source of  $\text{NO}_x$  in a given area [21,22]. Based on the analysis of seasonal characteristics of  $\text{NO}_2$  columns in China during 1996 and 2010, we found the influence of anthropogenic emissions with time to be expanding from east to west in China. Figure 5 shows an example in the northwest of China. It is clear that the Great Band of Yellow River, Ningxia, and North of Gansu were dominated by natural sources between 1996 and 1998, with maximal  $\text{NO}_2$  columns occurring in summer. However, during 2003 to 2005 and 2008 to 2010, most grids in Ningxia and the Great Band of the Yellow River had a maximum  $\text{NO}_2$  column in winter. Between 2008 and 2010, these also

included the urban areas in North of Gansu. The change of the seasonal characteristics of the maximum  $\text{NO}_2$  columns indicates an expanding influence of the anthropogenic emissions in these areas, and also that the dominant source of  $\text{NO}_x$  emissions has changed from natural to anthropogenic.

## 2.2 Driving forces of the $\text{NO}_x$ emission changes

To investigate the driving forces for these huge changes of spatial-temporal patterns of  $\text{NO}_x$  emissions in China over the past 15 years we compared the relative changes of satellite  $\text{NO}_2$  observations with those of the anthropogenic  $\text{NO}_x$  emissions as well as other social, economic, and energy indexes (Figure 6). To avoid any interference from back

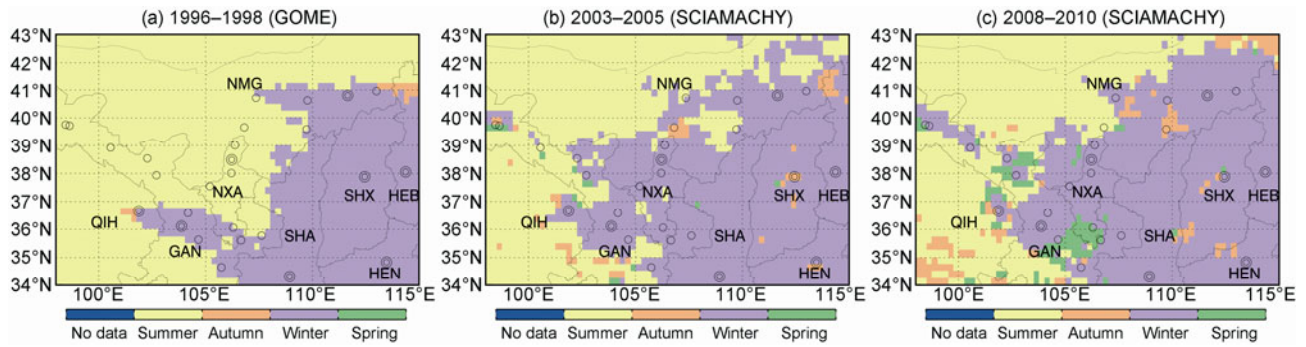


**Figure 5** Changes of seasonal NO<sub>2</sub> columns maxima over the central and west of China derived from two satellites (GOME and SCIAMACHY) (including Hebei (HEB), Henan (HEN), Shanxi (SHX), Shaanxi (SHA), Inner Mongolia (NMG), Ningxia (NXA), Gansu (GAN), and Qinghai (QIH)). Double circles denote the capitals of the provinces and single circles denote the major cities. Values are seasonal means for winter (December–February), spring (March–May), summer (June–August), and autumn (September–November).

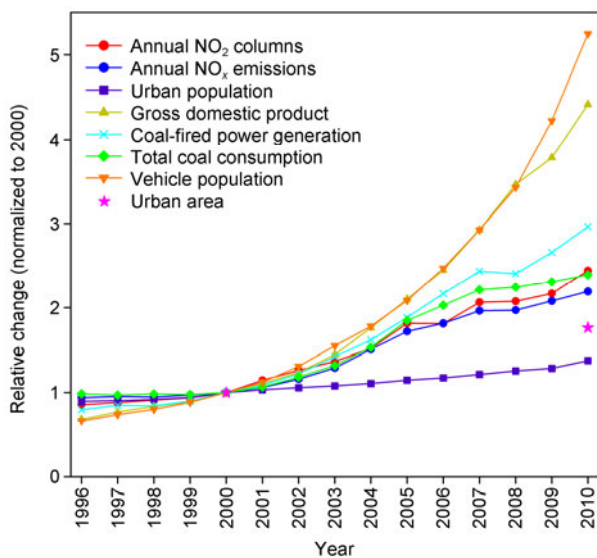


**Figure 6** Inter-annual relative changes in the NO<sub>2</sub> columns, anthropogenic NO<sub>x</sub> emissions, and social, economic, and energy indexes. All data were normalized to the year 2000. Study region: 30°–40°N, and 110°–123°E.

ground areas we conducted this comparison in the most polluted regions of China (East Central China, (ECC), 110°–123°E, and 30°–40°N). All of the data used in Figure 6 are from published statistical data sources. NO<sub>x</sub> emissions are updated to 2010 on the basis of our previous work, which took into account the impacts from technical evolution and emission control measures on the emission factors [4]. The bottom-up emission estimates suggest a 133% increase of the anthropogenic NO<sub>x</sub> emissions in ECC during 1996–2010, which is slightly lower than the 184% increase in the NO<sub>2</sub> columns measured by the satellites. Considering the uncertainties in emission estimates and satellite retrievals, and the inter-annual variations of the meteorological factors, these two growth rates actually agree well. The anthropogenic NO<sub>x</sub> emissions have increased dramatically since 2000, surging by a factor of 1.19 during 2000–2010.

This is comparable to the 144% increase in the NO<sub>2</sub> columns in this period and consistent with the rapid economic development in China since 2000.

The growths in coal consumption and vehicle ownership are usually considered as major driving forces of the Chinese increases in anthropogenic NO<sub>x</sub> emissions [4,23]. In Figure 6 the growth of the NO<sub>x</sub> emissions is consistent with that of total coal consumption, but is far less than that of vehicle ownership. Within the various indexes shown in Figure 6, the growth in the NO<sub>2</sub> columns has the best correlation (slope = 1.04,  $R^2 = 0.97$ ) with that of the total coal consumption. China has taken strict action to control vehicle emissions since 2000. These actions have resulted in the successful enforcement of the China III Emission Standard across the country. The new standard, the China IV Emission Standard is to be promoted soon. Therefore, although vehicle ownership has surged dramatically in the past decade, the vehicle emissions have not increased so significantly in recent years, and even decreased in some megacities [24]. The vehicle emissions are the major source of NO<sub>x</sub> in the megacities, so that the slowing of the growth in NO<sub>2</sub> columns measured by satellites in these megacities is mainly attributed to the effective control of vehicle emissions. These controls will continue for a long period to relieve the pressure from air pollution in megacities. NO<sub>x</sub> emissions in megacities in developed countries have already decreased because of the strict actions on vehicle emissions (see the case of Los Angeles in Figure 4).

In medium sized industrialized cities, coal consumption is still the major cause of NO<sub>x</sub> emissions. The controls of NO<sub>x</sub> emissions from coal-fired facilities are still at a preliminary stage in China. Although the low-nitrogen-burners have been popularized in large power plants, the national flue gas denitration program in power plants is not yet completed, and the NO<sub>x</sub> emissions from the industrial facilities are still not effectively controlled. Therefore, the rapid growth of NO<sub>x</sub> emissions in medium sized cities is largely related to the uncontrolled coal-fired emissions. It is worth noting that a large batch of power plants have been built in

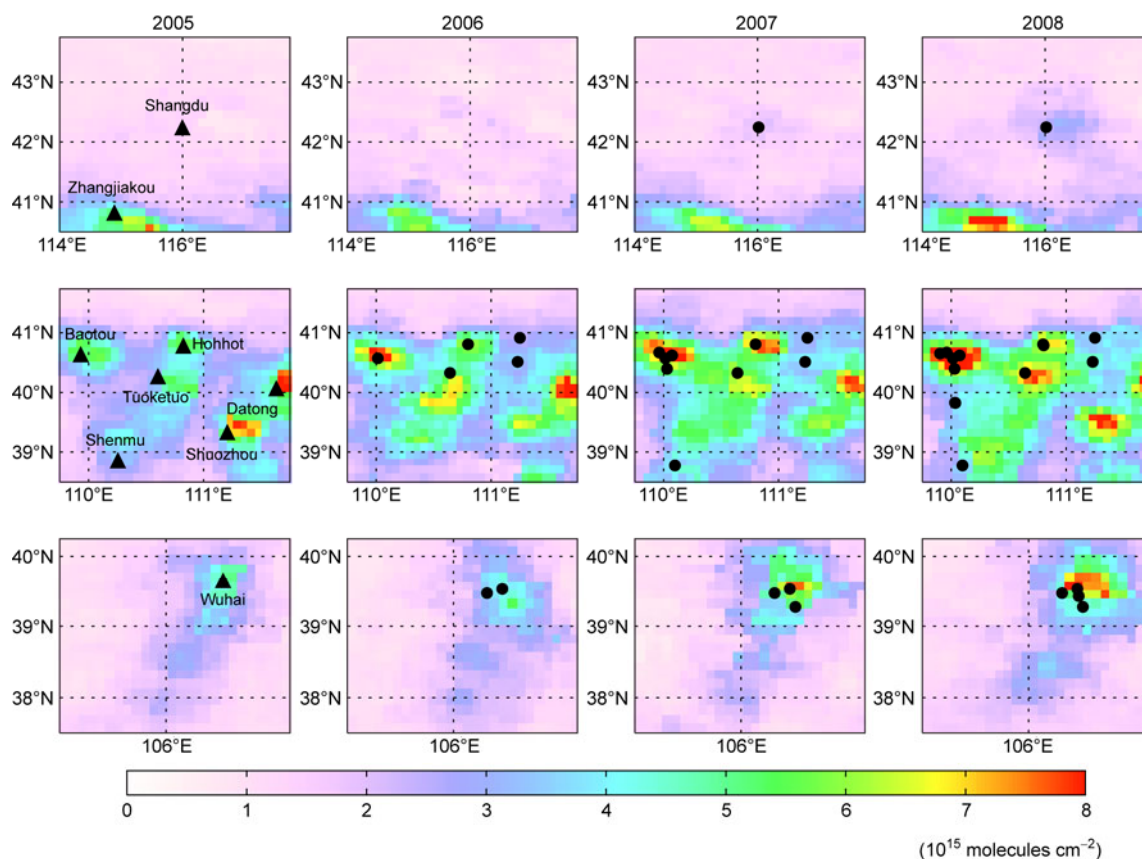


**Figure 7** Relationship between growth of  $\text{NO}_2$  columns and new power plants in Inner Mongolia. Solid circles denote the locations of new power plants which came into operation during 2005–2008.

recent years because of the urgent demands for electricity supply in the industrialization and urbanization processes, and these have severely aggravated the regional  $\text{NO}_x$  pollution. As shown in Figure 7, the  $\text{NO}_2$  columns increased more significantly close to the new power plants in Inner-Mongolia during 2005–2008. This indicates the importance of the transition of economic development patterns in key regions to control total coal consumption.

### 3 Conclusions

Over 1996–2010, we used satellite derived tropospheric  $\text{NO}_2$  columns over China from GOME and SCIAMACHY to study the spatial-temporal variations of  $\text{NO}_x$  emissions, as well as their driving forces. Results suggested that the existing high pollution regions have enlarged, and new ones have formed throughout the nation. Anthropogenic emission dominated regions have expanded from the east to central and western areas of China, with regional pollution characteristics increasingly significant. Analysis showed that the MEP-defined key regions in the “Joint Prevention and Control Strategy” are representative and rational. However, the highly polluted city-clusters in Central Henan and West of Shandong were not included in this Strategy, and the rapid

growth of  $\text{NO}_x$  emissions from industrial regions in Jilin and Inner Mongolia would possibly turn these two provinces into new highly polluted regions soon. We suggest considering these regions as top priorities in the next stage of the Strategy. Satellite observations also indicated that the growth rates of  $\text{NO}_x$  emissions in megacities have slowed in recent years, possibly because of effective controls on vehicle emissions. However,  $\text{NO}_x$  emissions are soaring in medium sized cities, largely attributed to uncontrolled emissions from coal-fired facilities.

*This work was supported by the National Basic Research Program of China (2010CB951803), the China Sustainable Energy Program (G-1010-12447) and the Project of Monitoring and Management on Emission Reduction, managed by the Ministry of Environmental Protection of China (2011A078).*

- 1 He K, Huo H, Zhang Q. Urban air pollution in China: Current status, characteristics, and progress. *Annu Rev Energy Environ*, 2002, 27: 397–431
- 2 Zhou W, Wang X, Zhang Y, et al. Current status of nitrogen oxides related pollution in China and integrated control strategy (in Chinese). *Acta Sci Nat Univ Pekin*, 2008, 44: 323–330
- 3 Ohara T, Akimoto H, Kurokawa J, et al. An Asian emission inventory of anthropogenic emission sources for the period 1980–2020. *Atmos Chem Phys*, 2007, 7: 4419–4444

- 4 Zhang Q, Streets D G, He K, et al. NO<sub>x</sub> emission trends for China, 1995–2004: The view from the ground and the view from space. *J Geophys Res*, 2007, 112
- 5 Zhang Q, Streets D G, Carmichael G R, et al. Asian emissions in 2006 for the NASA INTEX-B mission. *Atmos Chem Phys*, 2009, 9: 5131–5153
- 6 Streets D G, Bond T C, Carmichael G R, et al. An inventory of gaseous and primary aerosol emissions in Asia in the year 2000. *J Geophys Res*, 2003, 108
- 7 Martin R V. Satellite remote sensing of surface air quality. *Atmos Environ*, 2008, 42: 7823–7843
- 8 Fishman J, Bowman K W, Burrows J P, et al. Remote sensing of tropospheric pollution from space. *Bull Am Met Soc*, 2008, 89: 805–821
- 9 Martin R V, Jacob D J, Chance K, et al. Global inventory of nitrogen oxide emissions constrained by space-based observations of NO<sub>2</sub> columns. *J Geophys Res*, 2003, 108
- 10 Richter A, Burrows J P, Nüß H, et al. Increase in tropospheric nitrogen dioxide over China observed from space. *Nature*, 2005, 437: 129–132
- 11 Zhang X, Zhang P, Zhang Y, et al. Analysis of spatio-temporal variation of tropospheric NO<sub>2</sub> column and its source over China in recent 10-a. *Sci China Ser D: Earth Sci*, 2007, 37: 1409–1416
- 12 Yu H, Wang P, Zong X, et al. Satellite remote sensing of the variations of NO<sub>2</sub> column over Beijing during the Olympic Games. *Chin Sci Bull*, 2009, 54: 299–304
- 13 Tian H, Wang Y, Zhao D, et al. Formation and causes of NO<sub>x</sub> pollution on the east side of the Taihang Mountains in China. *Chin Sci Bull*, 2011, 56: 1464–1469
- 14 Boersma K F, Eskes H J, Brinksma E J. Error analysis for tropospheric NO<sub>2</sub> retrieval from space. *J Geophys Res*, 2004, 109
- 15 Beirle S, Platt U, Wenig M, et al. Weekly cycle of NO<sub>2</sub> by GOME measurements: A signature of anthropogenic sources. *Atmos Chem Phys*, 2003, 3: 2225–2232
- 16 Akimoto H, Ohara T, Kurokawa J, et al. Verification of energy consumption in China during 1996–2003 by using satellite observational data. *Atmos Environ*, 2006, 40: 7663–7667
- 17 Dikty S, Richter A, Weber M, et al. GOME-2 optical degradation as seen in level 2 data time series (2007–2010; BrO, NO<sub>2</sub>, HCHO, H<sub>2</sub>O, and O<sub>3</sub>), presented on EGU General Assembly 2011
- 18 Burrows J P, Weber M, Buchwitz M, et al. The global ozone monitoring experiment (GOME): Mission concept and first scientific results. *J Atmos Sci*, 1999, 56: 151–175
- 19 Bovensmann H, Burrows J P, Buchwitz M, et al. SCIAMACHY: Mission objectives and measurement modes. *J Atmos Sci*, 1999, 56: 127–150
- 20 MEP. Guiding Opinions on Facilitating the Joint Prevention and Control of Air Pollution and Improving the Regional Air Quality, 2010
- 21 van der A R J, Peters D H M U, Eskes H, et al. Detection of the trend and seasonal variation in tropospheric NO<sub>2</sub> over China. *J Geophys Res*, 2006, 111
- 22 van der A R J, Eskes H J, Boersma K F, et al. Trends, seasonal variability and dominant NO<sub>x</sub> source derived from a ten-year record of NO<sub>2</sub> measured from space. *J Geophys Res*, 2008, 113
- 23 Hao J M, Tian H Z, Lu Y Q. Emission inventories of NO<sub>x</sub> from commercial energy consumption in China, 1995–1998. *Environ Sci Technol*, 2002, 36: 552–560
- 24 Wang H, Fu L, Zhou Y, et al. Trends in vehicular emissions in China's mega cities from 1995 to 2005. *Environ Pollut*, 2010, 158: 394–400

**Open Access** This article is distributed under the terms of the Creative Commons Attribution License which permits any use, distribution, and reproduction in any medium, provided the original author(s) and source are credited.